Chinese Chemical Letters 34 (2023) 107566

Contents lists available at ScienceDirect

Chinese Chemical Letters

journal homepage: www.elsevier.com/locate/cclet

Self-assembly behavior of disaccharide-containing supra-amphiphiles

Zhenfei Gao[a], Tiannan Wang[a], Zikun Rao[a], Hui Yan[c], Ran Zhang[b,*], Guosong Chen[a,*]

[a] The State Key Laboratory of Molecular Engineering of Polymers and Department of Macromolecular Science, Fudan University, Shanghai 200433, China
[b] Changchun Institute of Applied Chemistry, Chinese Academy of Sciences, Changchun 130022, China
[c] School of Pharmaceutical Sciences, Liaocheng University, Liaocheng 252059, China

ARTICLE INFO

Article history:
Received 4 November 2021
Revised 24 May 2022
Accepted 25 May 2022
Available online 28 May 2022

Keywords:
Supra-amphiphile
Disaccharide
Self-assembly
Dynamic covalent bond
Molecular dynamics simulation

ABSTRACT

In this paper, supra-amphiphilic compounds containing disaccharides and azobenzene ends have been constructed *via* dynamic covalent bond. It was found that the slight structural difference of the disaccharides made significant difference in the self-assembled morphologies. Namely, three kinds of azo-disaccharide supra-amphiphiles were found to assemble into different morphologies, with the only difference in chemical structure from the disaccharides. More importantly, the structural difference between the disaccharides, including lactoside, maltoside and cellobioside was trivial. Molecular simulation revealed the packing of molecules was due to the different contribution from hydrogen bonds. The above results clearly indicated the contribution of saccharide packing, especially the related hydrogen bonding, to the final morphology of the assembled structures.

Supra-amphiphiles, distinguished from amphiphiles, are constructed by dynamic covalent bonds or non-covalent interactions [1,2], such as hydrogen bond, π-π interaction, host-guest conjugation and charge transfer interaction [3–7]. Supra-amphiphiles can be easily constructed through controlled manner, but compared with ordinary amphiphiles, they are much more tending to self-assemble even under very low concentrations due to the participation of dynamic interactions [8]. Therefore, developing the supra-amphiphiles can enrich the preparation of complex self-assemblies [9]. Meanwhile, in order to obtain the microscopic properties of the assemblies, many modern experimental methods including TEM, SEM and AFM have been widely used [1–4,10]. In recent years, due to the substantial increase in computing power, there have been many reports on the use of Monte Carlo (MC) and molecular dynamics (MD) simulation methods to study microscopic properties [11–14]. These kinds of researches provide in-depth information about dynamics and structural properties at the microscopic level.

It is known that the chemical structures of saccharides are complex and the variation between different saccharides could be trivial. However, such trivial difference could lead to significant property difference when the saccharides were polymerized and even bulk materials were formed. A most typical example is between starch and cellulose. Both of them are glucose-based macromolecules. The basic repeating unit of starch is maltose (α1–4-linked) and that of cellulose is cellobiose (β1–4-linked). Therefore, the structural difference between starch and cellulose only lies in different glycosidic bonds between glucoside units (α and β glycosidic bonds), which lead to completely different physiochemical properties. Moreover, the structural isomerism of disaccharides will affect their specific binding with proteins [15–18]. However, in most of the self-assembly studies, the contribution of saccharide structures has been more or less overlooked. Thus, it is demanding to construct saccharides-containing amphiphilic molecules and study their self-assembly behaviors in a relatively systematic manner. For this purpose, supra-amphiphile could be a choice since different saccharides could be installed to the same hydrophobic moieties *via* dynamic covalent bonding.

Herein, for the first time, the disaccharide-containing supra-amphiphiles were constructed by arylhydrazone dynamic covalent bond to explore the possibility of controlling self-assembly behaviors by varying saccharide structures. Azobenzene, a common building block in supramolecular chemistry, was chosen as the model hydrophobic part. The three constructed supra-amphiphiles containing different disaccharides, including lactoside (Lac), cellobioside (Cel) and maltoside (Mal) were assembled using the same assembly method. We found that slight difference in chemical structure (Fig. 1) could induce drastic change in assembly morphology. Vesicles were observed for Azo-Lac. For Azo-Cel, the morphology was like a sunflower. For Azo-Mal, only some irregular assemblies have been observed. To understand the above results better, molecular dynamics simulations on three azo-disaccharide

* Corresponding authors.
E-mail addresses: rzhangciac@ciac.ac.cn (R. Zhang), guosong@fudan.edu.cn (G. Chen).

https://doi.org/10.1016/j.cclet.2022.05.080
1001-8417/

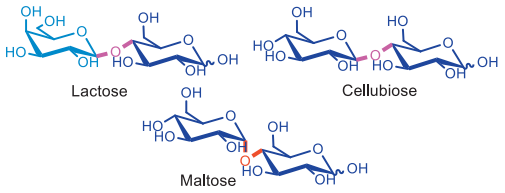

Fig. 1. The difference of chemical structure between three disaccharides: lactose, cellobiose and maltose. Light blue ring shows Galactose. Deep blue ring shows glucose. The α glycosidic bond shows as red, the β glycosidic bond shows as pink.

supra-amphiphiles were performed. It was found that the aggregation degree of the three disaccharides were shown in the sequence Mal > Cel > Lac due to their slight difference in the configurations, which can be employed to explain the assembly morphologies.

Three disaccharides with slight differences in configurations, which are lactoside (galactoside-(β1→4)-glucoside), maltoside (glucoside-(α1→4)-glucoside) and cellobioside (glucoside-(β1→4)-glucoside), were first employed to explore structural influence on assembled morphologies. As shown in Fig. 1, these three disaccharides are stereo-isomers. Both of Mal and Cel are based on glucosides, the only difference lies in the configuration of glycosidic bond, Mal with α-bond while Cel with β-bond. Although Lac is also connected by β-glycosidic bond, one of the repeating glucosides was changed to galactoside which contains axial OH group at C-4 instead of the equatorial OH of glucoside.

The synthetic procedures were shown in Scheme 1. Disaccharide-hydrazide was synthesized based on three disaccharides. Firstly, through the classical method of protecting hydroxyl groups on disaccharide, all hydroxyl groups were protected with acetyl groups (Ac-). Then the protected 1–hydroxyl group was deprotected by hydrazine acetate. Trichloroacetonitrile was used to activate the 1–hydroxyl group, followed by further reaction with ethyl 3-hydroxypropionate catalyzed by trimethylsilyl trifluoromethanesulfonate (TMSOTf) at −35 °C. The protective group of the hydroxyls was removed by hydrazine hydrate and disaccharide- hydrazide was finally obtained. After three kinds of disaccharide-hydrazide were synthesized, the Azo-CHO was synthesized from 4-hydroxybenzaldehyde and 4-phenylazophenol in 4 steps according to our previous works [18–21]. At last, mixing Azo-CHO and disaccharide- hydrazide at the molar ratio of 1:1 in DMSO for 4 days until the complete formation of azo-disaccharide

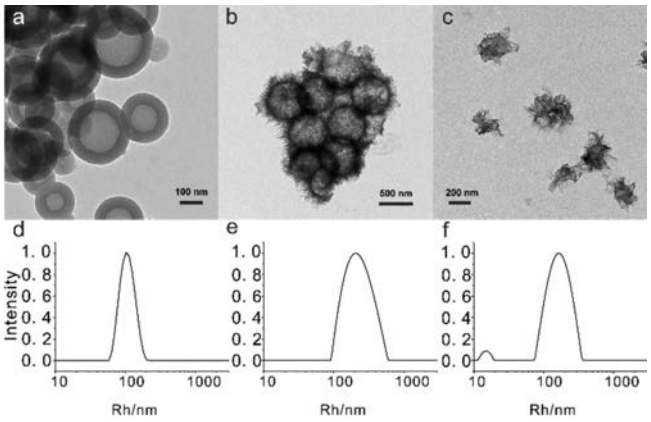

Fig. 2. The TEM images (a–c) and DLS images (d–f) of Azo-Lac, Azo-Cel, Azo-Mal.

and then stored as original solution, during which, ultrasound or heating was used to accelerate the formation speed [22]. The detailed synthetic procedures were reported in Supporting information.

The supra-amphiphile azo-disaccharide was assembled by a selective solvent method [22]. The self-assembly study of azo-disaccharide supra-amphiphile was performed in water. The self-assembled samples were prepared by adding 7.5 mL deionized water into 1 mL of azo-disaccharide (1 mg/mL in DMSO) under room temperature. Syringe pump was used, in order to maintain a constant dripping rate of 15 mm/h under vigorous stirring. Then the mixture was dialyzed (MWCO 1000) in deionized water to remove the extra DMSO. The final concentration of the samples was fixed at 0.1 mg/mL by adding deionized water. To visualize the morphologies of assemblies, TEM and DLS were used to characterize the morphologies. Tracking by TEM, vesicles with diameters of about 200–300 nm and wall thickness of about 50 nm was observed for Azo-Lac, indicating that a multi-layered vesicle structure has been obtained (Fig. 2a). The DLS analysis showed an average particle size of about 260 nm, which was consistent with the TEM results (Fig. 2d). For Azo-Cel, a surprising result was captured with TEM, *i.e.*, a sunflower-like morphology. It was a hollow spherical structure with a diameter ranging from 400 nm to 500 nm (Fig. 2b). The DLS result showed the particle size was about 406 nm, which

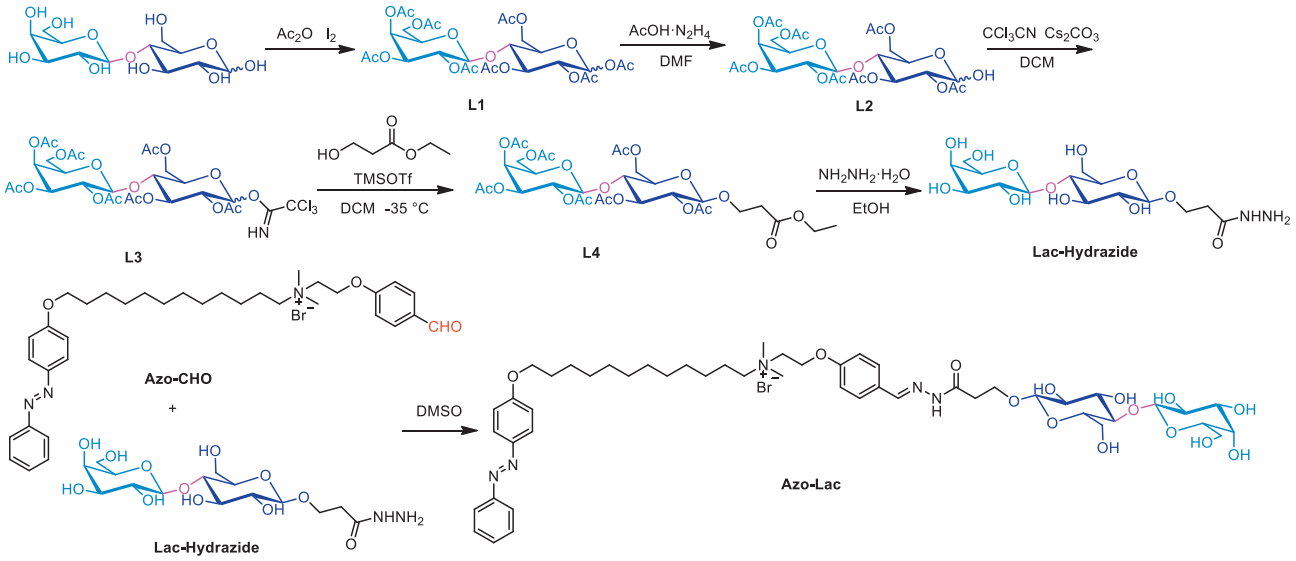

Scheme 1. Synthetic procedure of azo-disaccharide (Azo-Lac for example, Azo-Cel and Azo-Mal are shown in Supporting information).

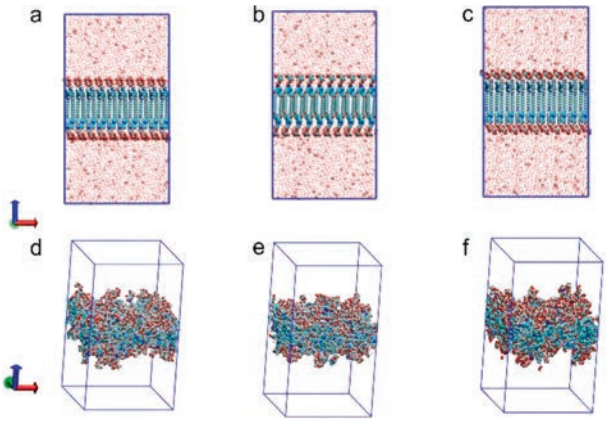

Fig. 3. Molecular dynamics simulations of bilayer formed by azo-disaccharide. (a–c) Side-view of initial bilayer for Azo-Lac, Azo-Cel and Azo-Mal. (d–f) Side-view of simulation results by Azo-Lac, Azo-Cel and Azo-Mal after relaxation for 20 ns, water molecules are hidden for clarity.

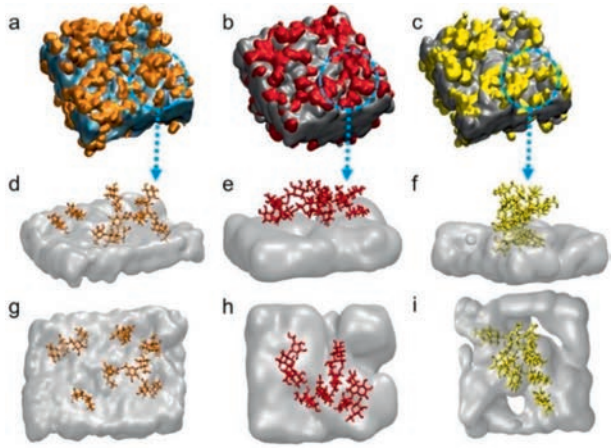

Fig. 4. Surface properties of bilayer MD simulation (a–c) Surface properties of Azo-Lac, Azo-Cel and Azo-Mal after relaxation for 20 ns. (d–f) Randomly selected configurations of the Azo-Lac, Azo-Cel and Azo-Mal molecules after relaxation for 20 ns. (g–i) Top-views of Figs. d–f. The disaccharide rings on the surface of Azo-Lac are shown in orange, the disaccharide rings on the surface of Azo-Cel are shown in red, and the disaccharide rings on the surface of Azo-Mal are shown in yellow.

was consistent with the TEM observations (Fig. 2e). As for Azo-Mal, the DLS result showed that there indeed existed assembly formation (Fig. 2f), but only some irregular structures were observed from TEM (Fig. 2c). It can be seen that the tiny differences between the three disaccharide-containing molecules have given three quite different morphologies of assemblies. From this point, the configurational isomerization effect should have a great influence on self-assembly behaviors.

The Azo-Lac, Azo-Cel and Azo-Mal in aqueous solution have shown completely different self-assembly behaviors. As discussed above, the only difference between these three supra-amphiphiles is the slight difference in the configuration of the disaccharide, Mal and Cel have different glycosidic bonds, and Lac is formed by a different glycoside with slight difference. So, it is important to have a deep insight into the relations between disaccharide conformation and the assembled morphologies. The theoretical and computational methods have always been expected in predicting the required structural features for specific applications and unveiling the mechanism behind. In this work, molecular dynamics simulations have been performed to investigate the assembly morphologies of our supra-amphiphiles.

For all three molecules, a pre-assembled lipid bilayer was constructed and placed in the center of a rectangular box with a dimension of $10 \times 10 \times 18\,nm^3$. Each lipid bilayer consisting of 100 molecules was constructed using Packmol program [23]. The disaccharide groups were initially set to point outward and the hydrophobic chains were set to point to the internal. Then, about 10,000 water molecules were filled into the vacuum at both sides of the bilayer. We constructed the initial structures of all lipid bilayers by mimicking the equilibrated and interleaved bilayer structure. The initial configurations of the three lipid bilayers were shown in Figs. 3a–c and their top views are shown in Figs. S1d–f (Supporting information). The structures of azo-disaccharide were shown in Figs. S1a–c (Supporting information). The simulations were performed using GROMACS package [24–27] with the CHARMM36 force field [28]. Water molecules were described using the simple point charge/extend (SPC/E) model [29]. The energy minimization was firstly performed for each system using the steep descent method. Then, 20 ns simulations under NPT ensemble were performed for the three systems at 298 K and 1 atm (the potential diagram see Fig. S2d in Supporting information). According to the classical method in simulating bilayer models, the semi-isotropic pressure coupling was applied during the simulation, in which the simulation box in z and x, y directions was rescaled individually [30,31].

The variations of the box lengths during the simulations were shown in Figs. S1g–i (Supporting information). The fluctuation of the data in Figs. S5g–i, showed that all systems had achieved equilibrium. The simulated side-view results of the azo-disaccharides were shown in Figs. 3d–f. At first glance, there were no evident differences among the three models. However, As described above, those three disaccharides show different conformations in water. And those differences in conformation may have a great influence on the spatial arrangement of disaccharide molecules. To further investigate the different assembly morphologies, the molecular surface model was shown for each model (Figs. 4a–c). The disaccharide rings of Azo-Lac are mainly evenly distributed on the surface of the bilayer, while the aggregations of Azo-Cel and Azo-Mal disaccharide rings are obvious, especially for the Azo-Mal model. Figs. 4d–i showed the detailed configuration of azo-disaccharides, which were selected randomly from the final configurations. It shows clearly that the disaccharide rings of Azo-Lac molecules distribute evenly and the distances among them are relatively large, indicating the weak interactions among the disaccharide rings. Whereas, the Azo-Cel and Azo-Mal molecules show obvious aggregation due to the strong interactions of disaccharide rings.

The interactions between disaccharide rings could be related to the hydrogen bonds. Under the same simulation protocol, the hydrogen bond numbers could provide distinguishable information. So, the number variations of hydrogen bonds during simulation time were counted to confirm the difference in their interactions (Fig. 5a). The number of hydrogen bonds in the three models remained stable during the last period of the simulation, which confirmed the equilibrium of the simulated models again. Obviously, the H–bond number of Azo-Mal was the largest, and the number of Azo-Lac was the lowest. The average number of hydrogen bonds on the surface of Azo-Lac, Azo-Cel and Azo-Mal are approximately 242, 279 and 327, respectively (Fig. 5b). In addition, the numbers of intramolecular and intermolecular hydrogen bonds in various azo-disaccharide bilayers were also counted. The final results showed that the number of intramolecular hydrogen bonds in the three azo-disaccharide bilayer models were almost the same. But the number of intermolecular hydrogen bonds between the three azo-disaccharide bilayers were quite different. The partially enlarged area also showed the same trend (Figs. S2a–c in Supporting information). The average number of intermolecular hydrogen bonds on the surface of Azo-Lac, Azo-Cel and Azo-Mal were approximately

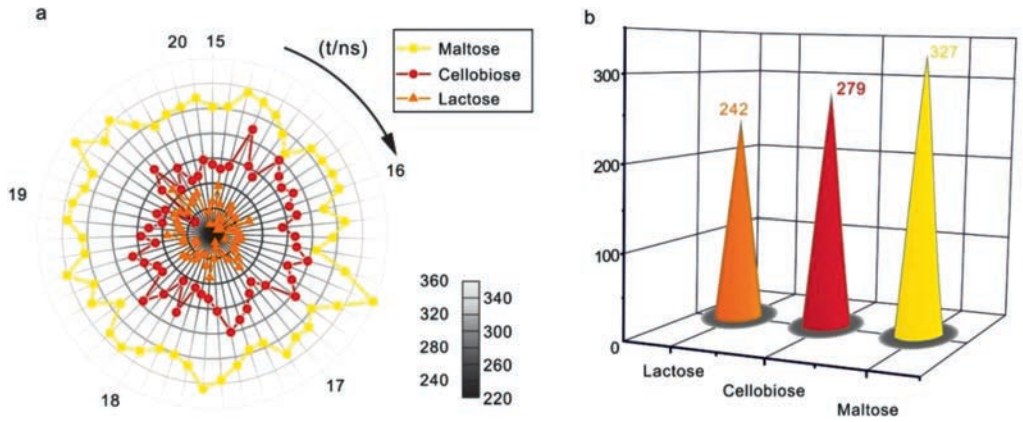

Fig 5. (a) Numbers of hydrogen bond plotted *versus* simulation time. (b) Average number of hydrogen bonds on the surface of Azo-Lac, Azo-Cel and Azo-Mal.

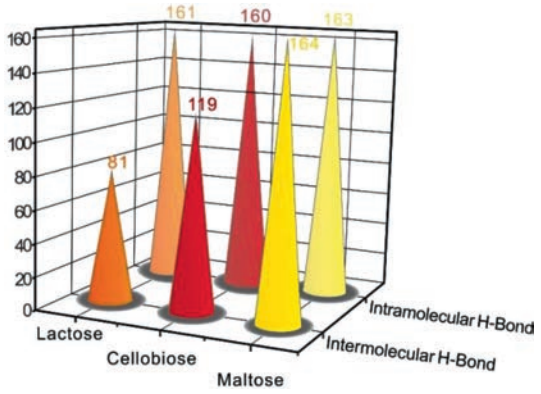

Fig 6. Numbers of intermolecular hydrogen bond and intramolecular hydrogen bond in Azo-Lac, Azo-Cel and Azo-Mal.

81, 119, and 164, respectively (Fig. 6). Therefore, we could infer that, due to the subtle difference in the configuration of the three azo-disaccharide, there was a huge difference in the number of intermolecular hydrogen bonds on their surface. The integral lifetime of the hydrogen bonds in the three azo-disaccharide bilayers was also calculated. The integral lifetime of Azo-Lac, Azo-Cel and Azo-Mal are approximately 201.71 ps, 228.47 ps and 265.22 ps, respectively (Table S1 in Supporting information). This indicated that, in Azo-Mal model, apart from displaying the largest number of H-bond, it also showed the strongest binding strength of H-bonds among the three amphiphiles. Therefore, even distribution of hydrogen bonds on the surface could lead to smoother surface in assemblies, and the greater the number of hydrogen bonds, the stronger the aggregation tendency. Based on those simulation results, Azo-Lac with fewer hydrogen bonds forms smooth vesicles, Azo-Cel with more hydrogen bonds has spikes on the surface of vesicles, and Azo-Mal, due to the strongest aggregation effect, is unable to form a regular morphology. It is consistent with the TEM data that Azo-Mal cannot give a regular morphology.

The morphology of each disaccharide molecule was also studied after the simulation reached equilibrium (Fig. S2 in Supporting information). In a Lac molecule, the galactoside and glucoside rings prefer to form a bent structure (Scheme 2), resulting in a relatively large steric hindrance. This bent structure facilitates the formation of intramolecular H-bonds between the galactoside and glucoside rings, leading to the formation of intramolecular hydrogen bond. Therefore, due to the bent structure, it is hard for two Lac molecules to interact with each other. In addition, the conformation of the Lac exhibits a prominent hydrophobic interface that is inclined to interact with the hydrophobic blocks *via* hydrophobicity. The Lac molecules prefer to distribute evenly at the surface. Whereas, the two adjacent glucoside rings of Mal tend to be coplanar, which facilitates intermolecular interactions among Mal molecules. Thus, the number of intermolecular hydrogen bonds increases, which also promotes the saccharide packing at the surface. As to Azo-Mal model, the two glucoside rings in a Cel molecule arranged crosswise. The steric hindrance strength of Cel molecule lies between Lac and Mal. So, the aggregation degree of Azo-Cel model is slightly lower than that of Azo-Mal model but higher than that of Azo-Lac model. Based on the above analysis, we plotted Scheme 2 to illustrate the relationship between the microstructure and macro morphology.

In the simulation part, we only paid attention to the influence of the disaccharide end on the morphology, but azobenzene can be transformed between *trans* and *cis* conformations by UV or visible light. Previous works by us and some other groups have proved the assembly of azobenzene-containing molecules can be rapidly regulated by photo-irradiation [32,33]. So, we expected possible morphology transformation upon irradiation of UV light. Under UV irradiation at 365 nm for 0.5 h, UV–vis spectroscopy was first used to investigate the photo responsiveness of the azo-disaccharide supra-amphiphile. The UV data showed that azobenzene part had been transformed from the stable *trans* conformation to the *cis* conformation after 0.5 h of UV light irradiation (Figs. S3c and d in Supporting information). Meanwhile, the morphology after irradiation was characterized by TEM (Figs. S3a and b in Supporting information). The UV data showed that when *cis*-azobenzene was irradiated by visible light, it returned to the *trans* conformation (Figs. S3e and f in Supporting information). The TEM and UV–vis results showed that UV light irradiation had no significant effect on the morphology of the two assemblies. This indicated the *cis* or *trans* conformations of the azobenzene group had no obvious influence on the morphologies, which also confirmed that the morphology of assemblies is mainly controlled by the disaccharide ends.

In summary, the assemblies of disaccharide-based supra-amphiphiles can be adjusted to diverse complex morphologies by varying the structures of disaccharide ends, which was demonstrated by both experiments and simulation. Three supra-amphiphiles with different disaccharides have been prepared, which present significant differences in assembly morphologies due to minor structural variations of disaccharides. Although the three disaccharides have similar chemical structures, they have very different self-assembly behavior. Simulation results revealed that a subtle structural change could greatly affect the related H-bond formation, then the packing of disaccharide molecule, finally the assembly morphology. The morphologies were greatly controlled by the packing of the disaccharide moieties.

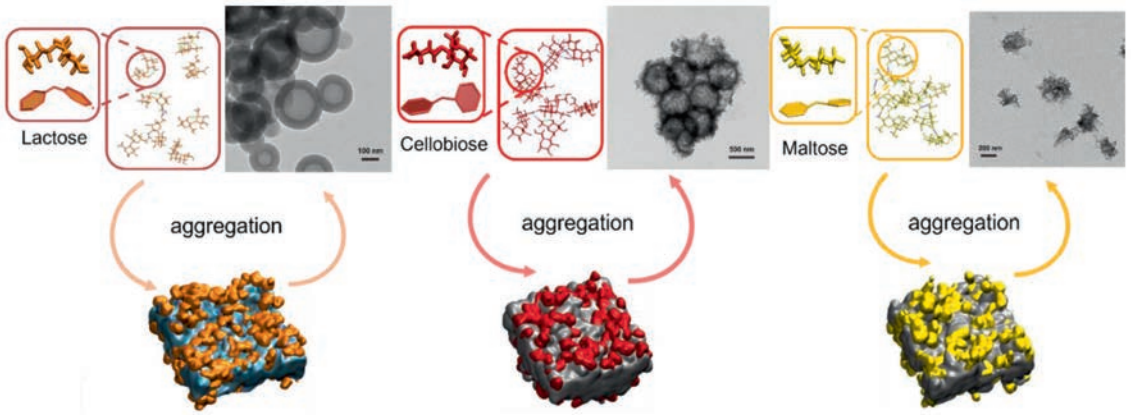

Scheme 2. The cartoon illustration of the self-assembly process of the azo-disaccharide supra-amphiphile.

Declaration of competing interest

The authors declare that they have no known competing financial interests or personal relationships that could have appeared to influence the work reported in this paper.

Acknowledgments

G. Chen thanks the National Natural Science Foundation of China (NSFC, Nos. 52125303, 51721002, 91956127 and 21975047) for financial support. R. Zhang thanks the National Natural Science Foundation of China (NSFC, Nos. 21674114 and 91956127) for financial support. This work is also supported by the Shanghai Municipal Science and Technology Major Project (No. 2018SHZDZX01) and ZJ Lab.

Supplementary materials

Supplementary material associated with this article can be found, in the online version, at doi:10.1016/j.cclet.2022.05.080.

References

[1] G.T. Wang, C. Wang, Z.Q. Wang, X. Zhang, Langmuir 27 (2011) 12375–12380.
[2] C. Wang, Z.Q. Wang, X. Zhang, Acc. Chem. Res. 45 (2012) 608–618.
[3] A.G. Slater, L.M.A. Perdigao, P.H. Beton, N.R. Champness, Acc. Chem. Res. 47 (2014) 3417–3427.
[4] T. Aida, E.W. Meijer, S.I. Stupp, Science 335 (2012) 813–817.
[5] T.R. Cook, Y.R. Zheng, P.J. Stang, Chem. Rev. 113 (2013) 734–777.
[6] H.T. Chifotides, K.R. Dunbar, Acc. Chem. Res. 46 (2013) 894–906.
[7] Z. Wu, J. Liu, Y. Li, et al., ACS Nano 9 (2015) 6315–6323.
[8] Q.Z. Zhou, H.J. Jiang, R. Chen, et al., Chem. Commun. 50 (2014) 10658–10660.
[9] H. Chen, M.H. Li, Chin. J. Polym. Sci. 37 (2019) 352–371.
[10] P.F. Sun, M.C. Lin, G.S. Chen, M. Jiang, Sci. China Chem. 59 (2016) 1616–1620.
[11] S.S. Jang, W.A. Goddard, J. Phys. Chem. B 110 (2006) 7992–8001.
[12] C.D. Bruce, M.L. Berkowitz, L. Perera, M.D.E. Forbes, J. Phys. Chem. B 106 (2002) 3788–3793.
[13] M. Tarek, D.J. Tobias, M.L. Klein, Phys. Chem. 99 (1995) 1393–1402.
[14] Y.L. Zhu, Z.Y. Lu, Acta Polym. Sin. 52 (2021) 884–897.
[15] L. Su, Y. Zhao, G.S. Chen, M. Jiang, Polym. Chem. 3 (2012) 1560–1566.
[16] X.M. Lian, D.X. Wu, X.H. Song, Macromolecules 43 (2010) 7434–7445.
[17] Z. Zhang, G.S. Chen, M. Jiang, Acta Polym. Sin. 52 (2021) 867–883.
[18] V. Biju, P.K. Sudeep, K.G. Thomas, et al., Langmuir 18 (2002) 1831–1839.
[19] L. Nagarapu, A.S Aneesa, G. Chandana, R. Bantu, J. Heterocycl. Chem. 46 (2009) 195–200.
[20] Y. Wang, N. Ma, Z. Wang, X. Zhang, Angew. Chem. Int. Ed. 46 (2007) 2823–2826.
[21] L. Su, C.M. Wang, et al., ACS Macro Lett. 3 (2014) 534–539.
[22] T.N. Wang, G. Yang, L.B. Wu, G.S. Chen, Chin. Chem. Lett. 27 (2016) 1740–1744.
[23] L. Martínez, R. Andrade, E.G. Birgin, J.M. Martínez, J. Comput. Chem. 30 (2009) 2157–2164.
[24] M.J. Abraham, T. Murtola, R. Schulz, et al., SoftwareX 6 (2015) 19–25.
[25] S. Páll, M.J. Abraham, C. Kutzner, B. Hess, E. Lindahl, Tackling exascale software challenges in molecular dynamics simulations with GROMACS, in: S. Markidis, E. Laure (Eds.), Solving Software Challenges for Exascale: International Conference on Exascale Applications and Software, EASC 2014, 8759, Springer, Cham, 2015, pp. 3–27.
[26] S. Pronk, S. Páll, R. Schulz, P. Larsson, Bioinformatics 29 (2013) 845–854.
[27] B. Hess, C. Kutzner, D. van der Spoel, E. Lindahl, J. Chem. Theory. Comput. 4 (2008) 435–447.
[28] A.D. MacKerell, D. Bashford, M. Bellott, et al., J. Phys. Chem. B 102 (1998) 3586–3616.
[29] H.J.C. Berendsen, J.R. Grigera, T.P. Straatsma, J. Phys. Chem. 91 (1987) 6269–6271.
[30] Z.W. Wang, RG. Larson, J. Phys. Chem. B 113 (2009) 13697–13710.
[31] Y.L. Feng, L. Li, Q.Q.G. Du, et al., CCS Chem. 3 (2021) 2570–2580.
[32] G.S. Kumar, D.C. Neckers, Chem. Rev. 89 (1989) 1915–1925.
[33] S. Malkin, E. Fischer, J. Phys. Chem. 66 (1962) 2482–2486.